

Article

Ionocovalency and Applications 1. Ionocovalency Model and Orbital Hybrid Scales

Yonghe Zhang

American Huilin Institute, 13810 Franklin Ave, Queens, NY 11355, USA;

E-Mail: y.zhang.huilin@gmail.com

Received: 27 September 2010; in revised form: 19 October 2010 / Accepted: 21 October 2010 /

Published: 3 November 2010

Abstract: Ionocovalency (IC), a quantitative dual nature of the atom, is defined and correlated with quantum-mechanical potential to describe quantitatively the dual properties of the bond. Orbital hybrid IC model scale, IC , and IC electronegativity scale, X_{IC} , are proposed, wherein the ionicity and the covalent radius are determined by spectroscopy. Being composed of the ionic function I and the covalent function C , the model describes quantitatively the dual properties of bond strengths, charge density and ionic potential. Based on the atomic electron configuration and the various quantum-mechanical built-up dual parameters, the model formed a *Dual Method* of the multiple-functional prediction, which has much more versatile and *exceptional* applications than traditional electronegativity scales and molecular properties. Hydrogen has *unconventional* values of IC and X_{IC} , lower than that of boron. The IC model can agree fairly well with the data of bond properties and satisfactorily explain chemical observations of elements throughout the Periodic Table.

Keywords: ionocovalency; molecular properties; electronegativity; theoretical chemistry

1. Introduction

In the valence-bond (VB) approach, the molecular wave function is written as a product of the state functions of the constituent atoms. This makes models based on the VB approximation intuitively appealing, as exemplified by the extreme usefulness of Lewis structures of “The Atom and the Molecule” [1] and by the wide acceptance of Pauling’s “Nature of the Chemical Bond” [2]. Before Lewis proposed his theory of the shared electron pair bond, bonding in some compounds could be

satisfactorily explained on the basis of simple electrostatic forces between the positive and negative ions which are assumed to be the basic molecular units. The shared electron pair bond is known as the covalent bond, while the other type is the ionic bond.

Over the years, the description of the properties of the covalent and ionic bond remains largely qualitative and Pauling's scale [3] due to not based on the electron configuration data, left a wide front for arguments and has led to many different suggestions for the bond strengths [4–24].

In the present work, we defined and correlated ionocovalency (*IC*), a quantitative atomic dual nature of ionicity and σ - and spatial-covalency with the quantum-mechanical potential to describe quantitatively the dual properties of bonds. Orbital hybrid *IC* scale and *IC* electronegativity X_{IC} scale are proposed wherein the ionicity and the covalent radius are determined by spectroscopy. Being composed of the ionic function *I* and the covalent function *C*, the model exhibits quantitatively the dual properties of bond strengths, charge density and ionic potential. Based on the atomic electron configuration, the quantum-mechanical built-up dual parameters and sub-models, which in turn exhibit various specific bond properties, the model formed a *Dual Method* of the multiple-functional prediction which has much more versatile and exceptional applications than traditional electronegativity scales and molecular properties. Hydrogen has its *unconventional* values lower than that of boron, residing on the borderline between the weak ionic and the weak covalent ions. The *IC* model can agree fairly well with the data of bond properties and satisfactorily explain chemical observations of elements throughout the Periodic Table.

2. Methodology

2.1. IC Model

Based on the VB approximation, the bond strengths can be considered mainly about the potential energy: the nuclear charge *Z* felt by valence electrons at the covalent boundary. And the term of Schrödinger's Wave Equation incorporating bond strength is the potential energy $Ze^2\psi/r$.

$$-\hbar^2\nabla^2\psi/8\pi^2m - Ze^2\psi/4\pi\epsilon_0r = E\psi \quad (2.1.1)$$

Ionic bonds are omnidirectional. The nuclear charge *Z* possesses the power of ionizing radiation and radiates positive charge in all directions. Therefore, the nuclear charge *Z* is directly proportional to the bond strengths but has the delocalized *ionic* nature.

The covalent radius, r_c is the other important part of the potential here. It is a distance from nucleus to a charge density wherein the bonding atoms are aligned and localized at very specific bond lengths, and it is inversely proportional to the bond strengths. In the case of the hydrogen atom, as Equation (2.1.1) shows, as the electron approaches the nucleus, the potential energy dives down toward minus-infinity, in order for the total energy *E* to remain constant, and its kinetic energy shoots up toward positive-infinity. So a compromise is reached in which theory tells us that the fall potential energy is just twice the kinetic energy, and the electron dances at an average distance that corresponds to the Bohr radius [25]. The calculation of the H₂ molecule by Heitler and London showed that as the inter-nuclear distance decreased, the potential energy associated with interactions between nucleus and electrons dropped very markedly until a minimum was reached, and then (owing to the greater effect of internuclear repulsion at much smaller internuclear distances) to rise sharply [26]. The minimum

corresponded fairly closely to the experimentally determined value of R , 0.74 Å (covalent radius = 0.37 Å, see below 4.2). Therefore, the covalent radius has the harmoniously localized *covalent* nature.

As atoms and molecules have the dual nature, ionocovalency, the bond strengths can be considered as a combination of the ionic and the covalent functions [10]. So the ionic function I can be considered as a function of the nuclear charge Z : $I(Z)$; and the covalent function C can be considered as a function of the covalent radius r_c : $C(r_c^{-1})$, wherein the reciprocal of r_c can be defined as *atomic covalency*.

Ionocovalently, the bond strengths and electronegativity, therefore, can be accounted for on the basis of the dual nature of bonds, and functionally defined as ionocovalency, a product of the ionic and the covalent functions:

$$IC = I(Z^*)C(r_c^{-1}) \quad (2.1.2)$$

And so the bond strengths, the potential energy and electronegativity have the IC framework of ionocovalency, which shows an effective ionocovalent potential, the attraction power that should be Pauling postulated.

According to the Bohr energy model

$$E = -Z^2 me^4 / 8n^2 h^2 \epsilon_0^2 = -RZ^2 / n^2 \quad (2.1.3)$$

we have derived *the effective nuclear charge* Z^* from ionization energy and the *effective principal quantum number* n^* [8,9]:

$$Z^* = n^*(I_z/R)^{1/2} \quad (2.1.4)$$

where I_z is the ultimate IE. R is the Rydberg constant, $R = 2\pi^2 \mu^4 2e^4 / h^2 = 13.6$ eV, h is Planck's constant. Substituting Equation (2.1.4) into (2.1.2), we can naturally correlate the bond properties to the quantum-mechanics, and get the IC model:

$$I(I_z)C(n^*r_c^{-1}) = n^*(I_{av}/R)^{1/2}r_c^{-1} \quad (2.1.5)$$

where the effective principal quantum number n^* is related to the electron energy, distribution and the distance from the nucleus. Hence, n^* can be considered as an energy of ionic function and also as a spatial distance of covalent function. The $n^*r_c^{-1}$, which is related to the spatial overlap, can be defined as *spatial-covalency* of covalent function (r_c^{-1} is a *linear- or σ -covalency*).

2.2. IC Electronegativity X_{IC}

As an application of ionocovalency, by Plotting Pauling values of X_p against $n^*(I_{av}/R)^{1/2}r_c^{-1}$, we obtain a new IC -potential electronegativity

$$X_{IC} = 0.412n^*(I_{av}/R)^{1/2}r_c^{-1} + 0.387 \quad (2.1.6)$$

Based on the above IC model, our previous electronegativity scale X_z [8,9] can be accounted for IC -force:

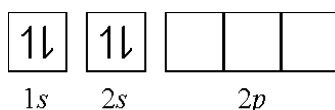
$$IC = I(V)C(r^{-1}) = I(Z^*)C(r^{-2}) = n^*(I_z/R)^{1/2}r_c^{-2} \quad (2.1.7)$$

$$X_z = 0.241n^*(I_z/R)^{1/2}r_c^{-2} + 0.775 \quad (2.1.8)$$

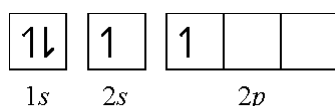
In Equation 2.1.5 and 2.1.6, I_{av} is *ionicity* (the average *IE* of valence shell electrons) determined by the following *IC orbital hybrid bonding procedures*. The diagrams are adapted from those in the excellent article by Blaber [27].

2.3. IC Orbital Hybrid Bonding Procedures

(1) **Ionization promotion:** As a valence shell fills, the successive increased ionization energy of an electron would provide the promotion energy for hybrid orbital formation e.g., consider gaseous molecules of BeF_2 . The fluorine atom has the electron configuration: $1s^2 2s^2 2p^5$. The beryllium atom has the electron configuration: $1s^2 2s^2$.



In the ground state, there are no unpaired electrons. However, the beryllium atom could obtain an unpaired electron by promoting an electron from the $2s$ orbital to the $2p$ orbital by its lower first *IE* (9.32 eV). The beryllium atom can now form two covalent bonds with fluorine atoms:

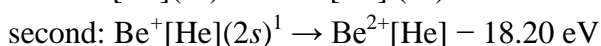


(2) **Ionicity hybridization:** We can combine functions for the $2s$ and $2p$ electrons to produce a “hybrid” orbital for both electrons. The charge transfer and charge distribution would occur from the higher energy level of the $2p$ orbital to the lower energy level of the $2s$ orbital to form an energy-lower and identical $2sp$ hybrid orbital. The ideas developed are adequate for calculation of the charge density identically distributed. The *IEs* of the $2s$ and $2p$ electrons can be averaged to result in a hybridizing *ionicity*, I_{av} :

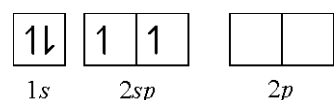
$$I_{av} = n^{-1} \sum_{i=1}^n I_i \quad (2.1.9)$$

where I_i is the *IE* of single electron of valence shell, n is number of valence shell electrons.

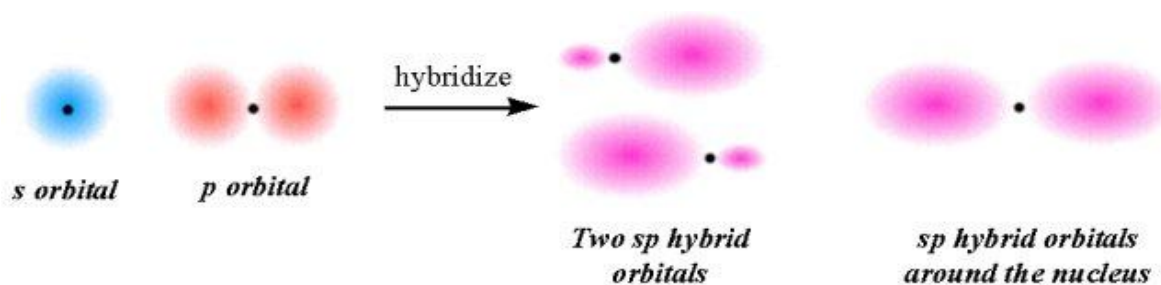
By Equation (2.1.9), we get an average *IE*: $I_{av} = 13.76$ eV from the first *IE* (9.32 eV) and second *IE* (18.2 eV):



of $2s$ electrons for $2p$ electrons:



(3) **Ionocovalency:** by localizing the hybridized ionicity at the covalent boundary r_c to form an ionocovalent bond of $2sp$ hybrid orbitals:



Hence, for beryllium, $IC = I(I_{av})C(n^*r_c^{-1}) = n^*(I_{av}/R)^{1/2}r_c^{-1} = 1.99(13.76/13.6)^{1/2}(0.970)^{-1} = 2.064$
 And $X_{IC} = 0.412 n^*(I_{av}/R)^{1/2}r_c^{-1} + 0.387 = 0.412*1.99(13.76/13.6)^{1/2}(0.970)^{-1} + 0.387 = 1.237$.

Similarly, an s orbital can also mix with all three p orbitals in the same subshell. For CH_4 by Equation (2.1.9), we get ionicity: $I_{av} = 37.015$ eV from the first IE (11.26 eV), second IE (24.40 eV), third IE (47.90 eV) and fourth IE (64.50 eV):

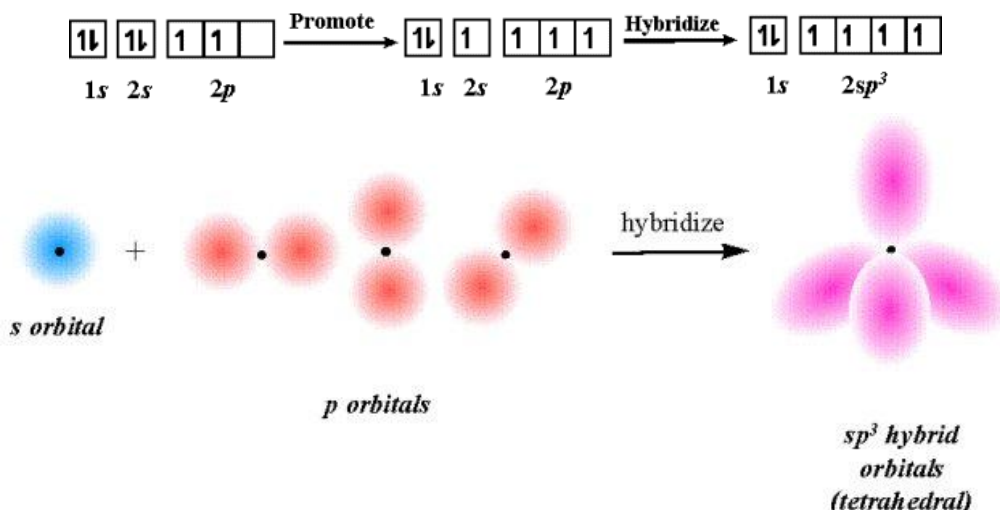
first: $\text{C}[\text{He}](2s)^2(2p)^2 \rightarrow \text{C}^+[\text{He}](2s)^2(2p)^1 - 11.26$ eV

second: $\text{C}^+[\text{He}](2s)^2(2p)^1 \rightarrow \text{C}^{2+}[\text{He}](2s)^2 - 24.40$ eV

third: $\text{C}^{2+}[\text{He}](2s)^2 \rightarrow \text{C}^{3+}[\text{He}](2s)^1 - 47.90$ eV

fourth: $\text{C}^{3+}[\text{He}](2s)^1 \rightarrow \text{C}^{4+}[\text{He}] - 64.50$ eV

of the all $2s$ and $2p$ electrons and form $2sp^3$ hybrid orbitals:



The IE is taken from Mackay *et al.* [28], the covalent radius r_c , is taken from Pauling [29], Batsanov [30], Cordero *et al.* [31], Rappe *et al.* [32] and the effective principal quantum number n^* is from our previous work [8,9]. The ionocovalency scale, IC , calculated from Equation (2.1.5) is listed in Chart 1 and the electronegativity scale, X_{IC} calculated from Equation (2.1.6) are listed in Table 1.

Based on the IC model, ionocovalency can be finally defined as “the effective potential caused by the ionicity on a bonding pair of electrons at the localized covalent boundary in different valence hybrid orbital states, forming an ionocovalent charge density”.

3. Results

3.1. General Trend of Periodic Table

Natural Values: Chart 1 shows that IC has a same value range as that of its atomic core charge. This phenomenon is particularly noticeable for the top period elements which have not yet experienced

much shielding effects. The atomic core charge is an effective nuclear charge and is always markedly less than the actual nuclear charge Z , but, as the shielding is not perfect, the core charge increases as Z increases, but more slowly. In the IC model, the effective nuclear charge is determined by natural IE , not from the calculation by shielding constants.

Ionocovalent Continuum: Chart 1 and Table 1 show that the ionocovalency IC and the electronegativity X_{IC} exhibit evidently the ionocovalency character. The greater the IC and the X_{IC} , the more covalent and the less ionic the cation is, and *vice versa*. Generally, across the period, the more right-hand-side an element is, the more covalent it is. And the more down-ward an element is, the more ionic it is. The IC and X_{IC} increase from the lower left to the upper right of the Periodic Table across the s and p blocks, and decrease down most columns. Trends parallel periodic trends in IE .

The ionocovalency is a continuum which is certainly an improvement over the old ionic-*versus*-covalent dichotomy. In so-called ‘pure’ ionic bonding, an electron is transferred completely from one atom to another, once this transfer is complete, the IC potential will act to try to pull this electron back to its parent ion. If IC partially succeeds then there will be some electron density, $n^*(I_{av}/R)^{1/2}r_c^{-1}$, in the region in between the ions, which is the situation in a covalent bond. Thus ‘pure’ ionic and ‘pure’ covalent bonds could be seen as two extremes of an IC continuum. And so a covalent scale has the ionic degree.

Energy-lowered Hybrid Bonding: The ionocovalent bonding procedures runs a charge promotion, charge distribution and energy-lowered hybrid sequence. Using Equation 2.1.5. and 2.1.6., we get the energy-lowered hybrid IC and X_{IC} values which are evidently lower than that of unhybridized values. For example, for carbon we have the energy-lowered $2sp^3$ hybrid $IC = 4.320$ and $X_{IC} = 2.167$. In the unhybridized situation, IC would be as higher as 5.702 and all unhybridized conventional electronegativities are as higher as than 2.5 for carbon.

Table 1. Atomic parameters.

Atm.No	Cations	n^*	I_z	I_{av}	r_c^{-1}	$n^*r_c^{-1}$	Z^*	r_c	X_z	X_{IC}	IC
1	H ⁺	0.85	13.600	13.600	2.703	2.297	0.850	0.370	2.271	1.333	2.297
2	He ²⁺	0.85	54.400	39.500	3.571	3.036	1.449	0.280	6.001	2.518	5.173
3	Li ⁺	1.99	5.3900	5.3900	0.816	1.624	1.253	1.225	0.976	0.808	1.023
4	Be ²⁺	1.99	18.200	13.760	1.031	2.052	2.002	0.970	1.365	1.237	2.064
5	B ³⁺	1.99	37.900	23.800	1.250	2.488	2.633	0.800	2.026	1.743	3.291
6	C ⁴⁺	1.99	64.500	37.015	1.316	2.618	3.283	0.760	2.583	2.167	4.320
6	C ³⁺	1.99	47.900	27.853	1.316	2.618	2.848	0.760	2.333	1.931	3.747
6	C ²⁺	1.99	24.400	17.830	1.316	2.618	2.279	0.760	1.887	1.622	2.998
7	N ⁵⁺	1.99	97.900	53.406	1.351	2.689	3.943	0.740	3.125	2.583	5.329
7	N ⁴⁺	1.99	77.500	42.283	1.351	2.689	3.509	0.740	2.866	2.341	4.742
7	N ³⁺	1.99	47.500	30.543	1.351	2.689	2.982	0.740	2.412	2.047	4.030
7	N ²⁺	1.99	29.600	22.065	1.351	2.689	2.535	0.740	2.067	1.798	3.425
7	N ⁺	1.99	14.530	14.530	1.351	2.689	2.057	0.740	1.680	1.532	2.780
8	O ⁶⁺	1.99	138.00	72.020	1.370	2.726	4.579	0.730	3.642	2.972	6.273
8	O ²⁺	1.99	35.100	24.360	1.370	2.726	2.663	0.730	2.221	1.890	3.648

Table 1. Cont.

9	F ⁷⁺	1.99	185.00	94.030	1.408	2.803	5.233	0.710	4.284	3.423	7.370
10	Ne ⁴⁺	1.99	97.100	55.785	1.724	3.431	4.030	0.580	4.584	3.250	6.949
10	Ne ²⁺	1.99	41.000	31.270	1.724	3.431	3.018	0.580	3.250	2.530	5.203
11	Na ⁺	2.89	5.1400	5.1400	0.636	1.838	1.777	1.572	0.948	0.853	1.130
12	Mg ²⁺	2.89	15.000	11.325	0.733	2.119	2.637	1.364	1.168	1.184	1.933
13	Al ³⁺	2.89	28.500	17.763	0.826	2.388	3.303	1.210	1.464	1.512	2.730
13	Al ⁺	2.89	5.9900	5.9900	0.826	2.388	1.918	1.210	1.091	1.040	1.585
14	Si ⁴⁺	2.89	45.100	25.763	0.847	2.449	3.978	1.180	1.686	1.776	3.371
14	Si ²⁺	2.89	16.300	12.225	0.847	2.449	2.740	1.180	1.323	1.344	2.322
15	P ⁵⁺	2.89	65.000	35.358	0.935	2.701	4.660	1.070	2.105	2.181	4.355
15	P ⁴⁺	2.89	51.400	27.948	0.935	2.701	4.143	1.070	1.958	1.982	3.872
15	P ³⁺	2.89	30.200	20.130	0.935	2.701	3.516	1.070	1.682	1.741	3.286
15	P ⁺	2.89	10.490	10.490	0.935	2.701	2.538	1.070	1.309	1.364	2.372
16	S ⁶⁺	2.89	88.000	46.077	0.971	2.806	5.319	1.030	2.445	2.515	5.165
16	S ⁴⁺	2.89	47.300	28.940	0.971	2.806	4.216	1.030	1.999	2.073	4.093
16	S ²⁺	2.89	23.300	16.830	0.971	2.806	3.215	1.030	1.634	1.673	3.121
17	Cl ⁷⁺	2.89	114.00	58.381	1.010	2.919	5.988	0.990	2.832	2.879	6.048
17	Cl ⁵⁺	2.89	67.800	39.534	1.010	2.919	4.927	0.990	2.362	2.438	4.977
17	Cl ³⁺	2.89	39.600	25.457	1.010	2.919	3.954	0.990	1.988	2.032	3.994
17	Cl ⁺	2.89	12.970	12.970	1.010	2.919	2.822	0.990	1.469	1.562	2.851
18	Ar ⁴⁺	2.89	59.800	35.965	1.031	2.979	4.700	0.970	2.327	2.383	4.845
18	Ar ²⁺	2.89	27.600	21.680	1.031	2.979	3.649	0.970	1.830	1.937	3.762
19	K ⁺	3.45	4.3400	4.3400	0.513	1.769	1.949	1.950	0.899	0.799	0.999
20	Ca ²⁺	3.45	11.900	9.0050	0.576	1.987	2.807	1.736	1.033	1.053	1.617
21	Sc ³⁺	3.45	24.800	14.713	0.695	2.397	3.588	1.439	1.317	1.414	2.494
22	Ti ⁴⁺	3.45	43.300	22.805	0.755	2.606	4.468	1.324	1.621	1.777	3.374
22	Ti ³⁺	3.45	27.500	15.973	0.755	2.606	3.739	1.324	1.449	1.550	2.824
22	Ti ²⁺	3.45	13.600	10.210	0.755	2.606	2.989	1.324	1.249	1.317	2.258
23	V ⁵⁺	3.45	65.200	32.528	0.817	2.819	5.336	1.224	1.990	2.183	4.359
23	V ⁴⁺	3.45	46.700	24.360	0.817	2.819	4.617	1.224	1.803	1.941	3.772
23	V ³⁺	3.45	29.300	16.913	0.817	2.819	3.847	1.224	1.590	1.682	3.143
23	V ²⁺	3.45	14.700	10.720	0.817	2.819	3.063	1.224	1.352	1.418	2.502
23	V ⁺	3.45	6.7400	6.7400	0.817	2.819	2.429	1.224	1.166	1.205	1.984
24	Cr ⁶⁺	3.45	90.600	43.878	0.853	2.944	6.197	1.172	2.337	2.565	5.287
24	Cr ⁵⁺	3.45	69.300	34.534	0.853	2.944	5.498	1.172	2.141	2.320	4.691
24	Cr ⁴⁺	3.45	49.100	25.843	0.853	2.944	4.756	1.172	1.925	2.059	4.058
24	Cr ³⁺	3.45	31.000	18.090	0.853	2.944	3.979	1.172	1.689	1.786	3.395
24	Cr ²⁺	3.45	16.500	11.635	0.853	2.944	3.191	1.172	1.442	1.509	2.723
24	Cr ⁺	3.45	6.7700	6.7700	0.853	2.944	2.434	1.172	1.202	1.243	2.077
25	Mn ⁷⁺	3.45	119.00	56.334	0.856	2.954	7.022	1.168	2.578	2.864	6.012
25	Mn ⁶⁺	3.45	95.000	45.890	0.856	2.954	6.337	1.168	2.386	2.622	5.426
25	Mn ⁵⁺	3.45	72.400	36.068	0.856	2.954	5.618	1.168	2.181	2.369	4.810
25	Mn ⁴⁺	3.45	51.200	26.985	0.856	2.954	4.860	1.168	1.958	2.101	4.161
25	Mn ³⁺	3.45	33.700	18.913	0.856	2.954	4.068	1.168	1.734	1.822	3.483
25	Mn ²⁺	3.45	15.600	11.520	0.856	2.954	3.175	1.168	1.428	1.507	2.719

Table 1. Cont.

25	Mn ⁺	3.45	7.4400	7.4400	0.856	2.954	2.552	1.168	1.226	1.287	2.185
26	Fe ⁶⁺	3.45	99.000	47.262	0.858	2.961	6.431	1.165	2.428	2.661	5.520
26	Fe ⁵⁺	3.45	75.000	36.914	0.858	2.961	5.684	1.165	2.214	2.397	4.879
26	Fe ⁴⁺	3.45	54.800	27.393	0.858	2.961	4.896	1.165	2.005	2.119	4.203
26	Fe ³⁺	3.45	30.700	18.257	0.858	2.961	3.997	1.165	1.695	1.801	3.431
26	Fe ²⁺	3.45	16.200	12.035	0.858	2.961	3.245	1.165	1.444	1.535	2.786
26	Fe ⁺	3.45	7.8700	7.8700	0.858	2.961	2.624	1.165	1.241	1.315	2.253
27	Co ⁴⁺	3.45	51.300	27.440	0.870	3.000	4.901	1.150	1.996	2.143	4.261
27	Co ³⁺	3.45	33.500	19.487	0.870	3.000	4.130	1.150	1.762	1.867	3.591
27	Co ²⁺	3.45	17.100	12.480	0.870	3.000	3.305	1.150	1.480	1.571	2.874
27	Co ⁺	3.45	7.8600	7.8600	0.870	3.000	2.623	1.150	1.253	1.327	2.281
28	Ni ⁴⁺	3.45	54.900	28.985	0.901	3.108	5.037	1.110	2.131	2.256	4.537
28	Ni ³⁺	3.45	35.200	20.347	0.901	3.108	4.220	1.110	1.861	1.953	3.802
28	Ni ²⁺	3.45	18.200	12.920	0.901	3.108	3.363	1.110	1.556	1.635	3.029
28	Ni ⁺	3.45	7.6400	7.6400	0.901	3.108	2.586	1.110	1.281	1.347	2.330
29	Cu ³⁺	3.45	36.800	21.610	0.901	3.108	4.349	1.110	1.885	2.001	3.918
29	Cu ²⁺	3.45	20.300	14.015	0.901	3.108	3.502	1.110	1.599	1.687	3.155
29	Cu ⁺	3.45	7.7300	7.7300	0.901	3.108	2.601	1.110	1.284	1.352	2.343
30	Zn ²⁺	3.45	18.000	13.695	0.801	2.762	3.462	1.249	1.388	1.529	2.772
30	Zn ⁺	3.45	9.3900	9.3900	0.801	2.762	2.867	1.249	1.218	1.333	2.295
31	Ga ³⁺	3.45	30.700	19.067	0.803	2.771	4.085	1.245	1.581	1.739	3.281
31	Ga ⁺	3.45	6.0000	6.0000	0.803	2.771	2.292	1.245	1.131	1.145	1.841
32	Ge ⁴⁺	3.45	45.700	25.925	0.818	2.821	4.763	1.223	1.794	1.992	3.895
32	Ge ²⁺	3.45	15.900	11.900	0.818	2.821	3.227	1.223	1.376	1.474	2.639
33	As ⁵⁺	3.45	62.600	33.902	0.826	2.851	5.447	1.210	1.993	2.242	4.502
33	As ³⁺	3.45	28.400	18.937	0.826	2.851	4.071	1.210	1.596	1.773	3.364
33	As ⁺	3.45	9.810	9.8100	0.826	2.851	2.930	1.210	1.257	1.385	2.422
34	Se ⁶⁺	3.45	81.700	42.442	0.855	2.949	6.095	1.170	2.264	2.533	5.209
34	Se ⁴⁺	3.45	42.900	26.163	0.855	2.949	4.785	1.170	1.854	2.072	4.090
34	Se ²⁺	3.45	21.200	15.480	0.855	2.949	3.681	1.170	1.533	1.683	3.146
35	Br ⁷⁺	3.45	103.00	52.601	0.876	3.021	6.785	1.142	2.529	2.835	5.941
35	Br ⁵⁺	3.45	59.700	35.322	0.876	3.021	5.560	1.142	2.111	2.393	4.869
35	Br ⁺	3.45	11.810	11.810	0.876	3.021	3.215	1.142	1.369	1.547	2.815
36	Kr ⁶⁺	3.45	78.500	45.200	0.862	2.974	6.290	1.160	2.260	2.621	5.422
36	Kr ⁴⁺	3.45	52.500	32.000	0.862	2.974	5.292	1.160	1.989	2.267	4.562
36	Kr ²⁺	3.45	24.500	19.250	0.862	2.974	4.105	1.160	1.604	1.845	3.538
37	Rb ⁺	3.85	4.1800	4.1800	0.463	1.782	2.134	2.160	0.885	0.794	0.988
38	Sr ²⁺	3.85	11.000	8.3500	0.522	2.011	3.017	1.914	1.003	1.036	1.576
39	Y ³⁺	3.85	20.500	13.027	0.619	2.382	3.768	1.616	1.211	1.348	2.332
40	Zr ⁴⁺	3.85	34.300	19.310	0.688	2.648	4.588	1.454	1.472	1.687	3.155
40	Zr ³⁺	3.85	23.000	14.313	0.688	2.648	3.950	1.454	1.346	1.506	2.716
40	Zr ²⁺	3.85	13.100	9.9700	0.688	2.648	3.296	1.454	1.206	1.321	2.267
41	Nb ⁵⁺	3.85	50.600	27.016	0.745	2.869	5.426	1.342	1.769	2.053	4.043
41	Nb ⁴⁺	3.85	38.300	21.120	0.745	2.869	4.798	1.342	1.640	1.860	3.575
41	Nb ³⁺	3.85	25.000	15.393	0.745	2.869	4.096	1.342	1.474	1.644	3.052

Table 1. Cont.

41	Nb ²⁺	3.85	14.300	10.590	0.745	2.869	3.397	1.342	1.303	1.430	2.532
41	Nb ⁺	3.85	6.8800	6.8800	0.745	2.869	2.738	1.342	1.141	1.228	2.040
42	Mo ⁶⁺	3.85	68.000	37.683	0.775	2.982	6.409	1.291	2.020	2.432	4.964
42	Mo ⁵⁺	3.85	61.200	31.620	0.775	2.982	5.870	1.291	1.956	2.260	4.547
42	Mo ⁴⁺	3.85	46.400	24.225	0.775	2.982	5.138	1.291	1.803	2.027	3.980
42	Mo ³⁺	3.85	27.200	16.833	0.775	2.982	4.283	1.291	1.562	1.754	3.318
42	Mo ²⁺	3.85	16.200	11.650	0.775	2.982	3.563	1.291	1.383	1.524	2.760
42	Mo ⁺	3.85	7.1000	7.1000	0.775	2.982	2.782	1.291	1.177	1.275	2.155
43	Tc ⁷⁺	3.85	94.000	46.297	0.787	3.031	7.103	1.270	2.287	2.691	5.593
43	Tc ⁶⁺	3.85	76.000	38.347	0.787	3.031	6.465	1.270	2.135	2.484	5.090
43	Tc ⁵⁺	3.85	59.000	30.816	0.787	3.031	5.795	1.270	1.973	2.267	4.563
43	Tc ⁴⁺	3.85	43.000	23.770	0.787	3.031	5.090	1.270	1.798	2.038	4.008
43	Tc ³⁺	3.85	29.500	17.360	0.787	3.031	4.350	1.270	1.622	1.798	3.425
43	Tc ²⁺	3.85	15.300	11.290	0.787	3.031	3.508	1.270	1.385	1.525	2.762
43	Tc ⁺	3.85	7.2800	7.2800	0.787	3.031	2.817	1.270	1.196	1.301	2.218
44	Ru ⁸⁺	3.85	119.00	57.771	0.806	3.102	7.935	1.241	2.557	3.021	6.394
44	Ru ⁷⁺	3.85	100.00	49.024	0.806	3.102	7.310	1.241	2.409	2.814	5.890
44	Ru ⁶⁺	3.85	81.000	40.528	0.806	3.102	6.646	1.241	2.245	2.593	5.355
44	Ru ⁵⁺	3.85	63.000	32.434	0.806	3.102	5.946	1.241	2.072	2.361	4.791
44	Ru ⁴⁺	3.85	46.500	24.793	0.806	3.102	5.198	1.241	1.889	2.113	4.189
44	Ru ³⁺	3.85	28.500	17.557	0.806	3.102	4.374	1.241	1.647	1.839	3.525
44	Ru ²⁺	3.85	16.800	12.085	0.806	3.102	3.629	1.241	1.445	1.592	2.924
45	Rh ⁶⁺	3.85	85.000	42.377	0.802	3.087	6.796	1.247	2.267	2.632	5.450
45	Rh ⁴⁺	3.85	45.600	25.565	0.802	3.087	5.279	1.247	1.868	2.131	4.233
45	Rh ³⁺	3.85	31.100	18.887	0.802	3.087	4.537	1.247	1.677	1.886	3.638
45	Rh ²⁺	3.85	18.100	12.780	0.802	3.087	3.732	1.247	1.463	1.620	2.993
45	Rh ⁺	3.85	7.4600	7.4600	0.802	3.087	2.851	1.247	1.217	1.329	2.287
46	Pd ⁶⁺	3.85	90.000	44.273	0.782	3.013	6.946	1.278	2.236	2.626	5.435
46	Pd ⁵⁺	3.85	66.000	35.128	0.782	3.013	6.188	1.278	2.026	2.382	4.842
46	Pd ⁴⁺	3.85	49.000	27.410	0.782	3.013	5.466	1.278	1.853	2.149	4.277
46	Pd ³⁺	3.85	32.900	20.210	0.782	3.013	4.693	1.278	1.659	1.900	3.672
46	Pd ²⁺	3.85	19.400	13.870	0.782	3.013	3.888	1.278	1.453	1.640	3.042
47	Ag ³⁺	3.85	34.600	21.227	0.747	2.875	4.810	1.339	1.600	1.867	3.592
47	Ag ²⁺	3.85	21.500	14.540	0.747	2.875	3.981	1.339	1.426	1.612	2.973
47	Ag ⁺	3.85	7.5800	7.5800	0.747	2.875	2.874	1.339	1.161	1.271	2.147
48	Cd ²⁺	3.85	16.900	12.945	0.708	2.725	3.756	1.413	1.293	1.482	2.658
48	Cd ⁺	3.85	8.9900	8.9900	0.694	2.674	3.130	1.440	1.139	1.283	2.174
49	In ³⁺	3.85	28.000	17.563	0.668	2.572	4.375	1.497	1.369	1.591	2.923
49	In ⁺	3.85	5.7900	5.7900	0.668	2.572	2.512	1.497	1.045	1.078	1.678
50	Sn ⁴⁺	3.85	40.700	23.285	0.715	2.752	5.038	1.399	1.595	1.871	3.601
50	Sn ²⁺	3.85	14.600	10.970	0.715	2.752	3.458	1.399	1.266	1.405	2.472
51	Sb ⁵⁺	3.85	55.500	30.028	0.709	2.730	5.721	1.410	1.718	2.059	4.057
51	Sb ³⁺	3.85	25.300	16.813	0.709	2.730	4.281	1.410	1.412	1.638	3.036
52	Te ⁶⁺	3.85	70.700	37.085	0.730	2.810	6.358	1.370	1.902	2.299	4.641
52	Te ⁴⁺	3.85	37.400	23.253	0.730	2.810	5.034	1.370	1.595	1.901	3.675

Table 1. Cont.

52	Te ²⁺	3.85	18.600	13.810	0.730	2.810	3.880	1.370	1.353	1.554	2.832
53	I ⁷⁺	3.85	92.344	46.535	0.750	2.886	7.122	1.334	2.134	2.587	5.339
53	I ⁵⁺	3.85	52.395	23.794	0.750	2.886	5.092	1.334	1.798	1.960	3.817
53	I ⁺	3.85	10.450	10.450	0.750	2.886	3.375	1.334	1.232	1.429	2.530
54	Xe ⁸⁺	3.85	112.91	55.46	0.714	2.750	7.775	1.400	2.139	2.675	5.553
54	Xe ⁶⁺	3.85	68.718	39.18	0.714	2.750	6.534	1.400	1.839	2.310	4.667
54	Xe ⁴⁺	3.85	43.956	27.35	0.714	2.750	5.459	1.400	1.626	1.994	3.900
54	Xe ²⁺	3.85	21.200	16.670	0.714	2.750	4.262	1.400	1.366	1.641	3.044
55	Cs ⁺	4.36	3.8900	3.8900	0.426	1.855	2.332	2.350	0.877	0.796	0.992
56	Ba ²⁺	4.36	10.000	7.6050	0.505	2.201	3.260	1.981	1.005	1.065	1.646
57	La ³⁺	4.36	19.200	11.960	0.534	2.330	4.089	1.871	1.132	1.287	2.185
58	Ce ⁴⁺	4.36	36.720	18.311	0.608	2.649	5.059	1.646	1.412	1.653	3.074
58	Ce ³⁺	4.36	20.199	12.174	0.608	2.649	4.125	1.646	1.248	1.420	2.506
59	Pr ⁴⁺	4.36	38.979	17.918	0.607	2.646	5.005	1.648	1.430	1.638	3.037
59	Pr ³⁺	4.36	21.619	10.898	0.607	2.646	3.903	1.648	1.263	1.363	2.368
60	Nd ⁴⁺	4.36	40.420	19.676	0.609	2.655	5.244	1.642	1.447	1.703	3.194
60	Nd ³⁺	4.36	22.075	12.762	0.609	2.655	4.223	1.642	1.272	1.447	2.572
60	Nd ²⁺	4.36	10.716	8.105	0.609	2.655	3.366	1.642	1.121	1.232	2.050
61	Pm ³⁺	4.36	22.283	12.914	0.613	2.675	4.249	1.630	1.281	1.461	2.606
62	Sm ³⁺	4.36	23.423	13.373	0.602	2.627	4.323	1.660	1.275	1.460	2.604
63	Eu ³⁺	4.36	24.874	13.929	0.541	2.357	4.412	1.850	1.190	1.370	2.385
63	Eu ²⁺	4.36	11.245	8.4570	0.541	2.357	3.438	1.850	1.054	1.153	1.858
64	Gd ³⁺	4.36	20.624	12.962	0.620	2.701	4.256	1.614	1.272	1.474	2.637
64	Gd ²⁺	4.36	12.126	9.1310	0.620	2.701	3.572	1.614	1.156	1.299	2.213
65	Tb ⁴⁺	4.36	39.798	19.759	0.628	2.739	5.255	1.592	1.484	1.747	3.301
65	Tb ³⁺	4.36	21.868	13.079	0.628	2.739	4.276	1.592	1.301	1.494	2.686
66	Dy ³⁺	4.36	22.801	13.466	0.629	2.744	4.339	1.589	1.314	1.512	2.730
67	Ho ³⁺	4.36	22.801	13.542	0.633	2.759	4.351	1.580	1.320	1.521	2.754
68	Er ³⁺	4.36	22.697	13.577	0.638	2.782	4.356	1.567	1.328	1.532	2.780
69	Tm ³⁺	4.36	23.671	13.970	0.640	2.791	4.419	1.562	1.343	1.553	2.829
69	Tm ²⁺	4.36	12.053	9.1190	0.640	2.791	3.570	1.562	1.180	1.329	2.286
70	Yb ³⁺	4.36	25.029	14.487	0.589	2.566	4.500	1.699	1.269	1.478	2.649
70	Yb ²⁺	4.36	12.178	9.2160	0.589	2.566	3.589	1.699	1.119	1.257	2.112
71	Lu ³⁺	4.36	20.956	13.423	0.598	2.609	4.332	1.671	1.242	1.455	2.592
72	Hf ⁴⁺	4.36	33.300	19.538	0.693	3.024	5.226	1.442	1.566	1.880	3.624
72	Hf ³⁺	4.36	23.300	14.950	0.693	2.024	4.571	1.442	1.436	1.693	3.170
72	Hf ²⁺	4.36	14.900	10.775	0.693	2.024	3.881	1.442	1.304	1.496	2.691
73	Ta ⁵⁺	4.36	45.000	24.898	0.745	3.246	5.899	1.343	1.835	2.197	4.393
73	Ta ⁴⁺	4.36	33.100	19.873	0.745	3.246	5.270	1.343	1.684	2.004	3.924
73	Ta ³⁺	4.36	22.300	15.463	0.745	3.246	4.649	1.343	1.521	1.813	3.462
73	Ta ²⁺	4.36	16.200	12.050	0.745	3.246	4.104	1.343	1.411	1.646	3.056
73	Ta ⁺	4.36	7.8900	7.8900	0.745	3.246	3.321	1.343	1.219	1.406	2.473
74	W ⁶⁺	4.36	61.000	32.363	0.770	3.356	6.726	1.299	2.094	2.520	5.178
74	W ⁵⁺	4.36	48.000	26.636	0.770	3.356	6.102	1.299	1.945	2.322	4.697
74	W ⁴⁺	4.36	35.400	21.295	0.770	3.356	5.456	1.299	1.780	2.117	4.200

Table 1. Cont.

74	W ³⁺	4.36	24.100	16.593	0.770	3.356	4.816	1.299	1.604	1.914	3.707
74	W ²⁺	4.36	17.700	12.840	0.770	3.356	4.236	1.299	1.485	1.731	3.261
75	Re ⁷⁺	4.36	79.000	40.311	0.782	3.412	7.506	1.278	2.326	2.807	5.874
75	Re ⁶⁺	4.36	64.000	33.863	0.782	3.412	6.880	1.278	2.171	2.605	5.383
75	Re ⁵⁺	4.36	51.000	27.836	0.782	3.412	6.238	1.278	2.021	2.398	4.881
75	Re ⁴⁺	4.36	37.700	22.045	0.782	3.412	5.551	1.278	1.846	2.177	4.344
75	Re ³⁺	4.36	26.000	16.827	0.782	3.412	4.850	1.278	1.665	1.950	3.795
75	Re ²⁺	4.36	16.600	12.240	0.782	3.412	4.136	1.278	1.486	1.720	3.237
75	Re ⁺	4.36	7.8800	7.8800	0.782	3.412	3.319	1.278	1.265	1.457	2.597
76	Os ⁸⁺	4.36	99.000	49.325	0.797	3.474	8.303	1.255	2.575	3.113	6.616
76	Os ⁷⁺	4.36	83.000	42.230	0.797	3.474	7.683	1.255	2.423	2.909	6.122
76	Os ⁶⁺	4.36	68.000	35.433	0.797	3.474	7.038	1.255	2.267	2.697	5.608
76	Os ⁵⁺	4.36	54.000	28.920	0.797	3.474	6.358	1.255	2.104	2.474	5.066
76	Os ⁴⁺	4.36	40.000	22.650	0.797	3.474	5.627	1.255	1.919	2.234	4.483
76	Os ³⁺	4.36	25.000	16.867	0.797	3.474	4.855	1.255	1.680	1.981	3.869
76	Os ²⁺	4.36	16.900	12.800	0.797	3.474	4.230	1.255	1.519	1.776	3.370
76	Os ⁺	4.36	8.7000	8.7000	0.797	3.474	3.487	1.255	1.309	1.532	2.779
77	Ir ⁶⁺	4.36	72.000	36.683	0.794	3.460	7.161	1.260	2.298	2.728	5.683
77	Ir ⁵⁺	4.36	57.000	29.620	0.794	3.460	6.434	1.260	2.130	2.491	5.107
77	Ir ⁴⁺	4.36	39.000	22.775	0.794	3.460	5.642	1.260	1.896	2.232	4.478
77	Ir ³⁺	4.36	27.000	17.367	0.794	3.460	4.927	1.260	1.708	1.998	3.910
77	Ir ²⁺	4.36	16.000	12.550	0.794	3.460	4.188	1.260	1.493	1.757	3.324
77	Ir ⁺	4.36	9.1000	9.1000	0.794	3.460	3.566	1.260	1.316	1.553	2.831
78	Pt ⁶⁺	4.36	75.000	37.867	0.775	3.380	7.275	1.290	2.258	2.711	5.640
78	Pt ⁵⁺	4.36	55.000	30.440	0.775	3.380	6.523	1.290	2.045	2.470	5.056
78	Pt ⁴⁺	4.36	41.100	24.300	0.775	3.380	5.828	1.290	1.873	2.248	4.518
78	Pt ³⁺	4.36	28.500	18.700	0.775	3.380	5.113	1.290	1.689	2.020	3.963
78	Pt ²⁺	4.36	18.600	13.800	0.775	3.380	4.392	1.290	1.513	1.790	3.405
78	Pt ⁺	4.36	9.0000	9.0000	0.775	3.380	3.547	1.290	1.289	1.520	2.749
79	Au ⁵⁺	4.36	58.000	32.346	0.749	3.263	6.724	1.336	1.991	2.461	5.033
79	Au ³⁺	4.36	30.500	20.077	0.749	3.263	5.297	1.336	1.657	2.021	3.965
79	Au ²⁺	4.36	20.500	14.865	0.749	3.263	4.558	1.336	1.498	1.793	3.412
79	Au ⁺	4.36	9.2300	9.2300	0.749	3.263	3.592	1.336	1.260	1.495	2.689
80	Hg ²⁺	4.33	18.800	14.620	0.694	3.008	4.490	1.440	1.367	1.672	3.118
80	Hg ⁺	4.36	10.440	10.440	0.694	3.028	3.820	1.440	1.219	1.480	2.653
81	Tl ⁺³	4.36	29.800	18.770	0.646	2.815	5.122	1.549	1.423	1.749	3.307
81	Tl ⁺	4.36	6.1100	6.1100	0.646	2.815	2.922	1.549	1.069	1.164	1.887
82	Pb ⁴⁺	4.36	42.300	24.180	0.650	2.835	5.814	1.538	1.558	1.944	3.780
82	Pb ²⁺	4.36	15.000	11.210	0.650	2.835	3.958	1.538	1.242	1.447	2.574
83	Bi ⁵⁺	4.36	56.000	30.178	0.658	2.868	6.495	1.520	1.698	2.147	4.273
83	Bi ⁺³	4.36	25.600	16.530	0.658	2.868	4.807	1.520	1.399	1.690	3.162
84	Po ⁶⁺	4.36	71.488	37.111	0.654	2.850	7.202	1.530	1.804	2.326	4.707
84	Po ⁴⁺	4.36	37.448	22.922	0.654	2.850	5.660	1.530	0.775	1.911	3.700
84	Po ³⁺	4.36	27.745	18.072	0.654	2.850	5.026	1.530	1.416	1.740	3.285
84	Po ²⁺	4.36	18.051	13.235	0.654	2.850	4.301	1.530	1.292	1.545	2.811

Table 1. Cont.

85	At ⁷⁺	4.36	88.291	44.345	0.690	3.007	7.873	1.450	2.048	2.624	5.430
85	At ⁵⁺	4.36	88.291	29.370	0.690	3.007	6.407	1.450	2.048	2.208	4.419
85	At ³⁺	4.36	29.262	18.660	0.690	3.007	5.107	1.450	1.508	1.838	3.522
85	At ⁺	4.36	9.2000	9.2000	0.690	3.007	3.586	1.450	1.186	1.406	2.473
86	Rn ⁸⁺	4.36	106.54	44.700	0.704	3.070	7.904	1.420	2.234	2.680	5.567
86	Rn ⁶⁺	4.36	65.490	36.730	0.704	3.070	7.165	1.420	1.919	2.466	5.046
86	Rn ⁴⁺	4.36	41.900	25.250	0.704	3.070	5.941	1.420	1.690	2.111	4.183
87	Fr ⁺	4.36	3.9800	3.9800	0.407	1.772	2.359	2.460	0.869	0.782	0.959
88	Ra ²⁺	4.36	10.200	7.740	0.426	1.855	3.289	2.350	0.940	0.964	1.400
89	Ac ³⁺	4.36	19.692	12.321	0.504	2.199	4.150	1.983	1.097	1.249	2.093
90	Th ⁴⁺	4.36	28.800	16.595	0.581	2.533	4.816	1.721	1.291	1.540	2.798
90	Th ³⁺	4.36	20.000	12.527	0.581	2.533	4.184	1.721	1.205	1.389	2.431
91	Pa ⁴⁺	4.36			0.584	2.548	3.900	1.711	1.096	1.326	2.279
92	U ⁴⁺	4.36			0.594	2.589	3.900	1.684	1.106	1.341	2.316
93	Np ⁴⁺	4.36			0.600	2.617	3.900	1.666	1.114	1.351	2.341
94	Pu ⁴⁺	4.36			0.604	2.631	3.900	1.657	1.117	1.357	2.354
95	Am ⁴⁺	4.36			0.602	2.627	3.900	1.660	1.116	1.355	2.349
96	Cm ³⁺	4.36			0.555	2.421	3.900	1.801	1.065	1.279	2.165
97	Bk ³⁺	4.36			0.568	2.476	3.900	1.761	1.078	1.299	2.215
98	Cf ³⁺	4.36			0.571	2.491	3.900	1.750	1.082	1.305	2.229
99	Es ³⁺	4.36			0.580	2.529	3.900	1.724	1.091	1.319	2.262
100	Fm ³⁺	4.36			0.584	2.547	3.900	1.712	1.096	1.326	2.278
101	Md ³⁺	4.36			0.592	2.581	3.900	1.689	1.104	1.338	2.309
102	No ³⁺	4.36			0.596	2.597	3.900	1.679	1.108	1.344	2.323
103	Lw ³⁺	4.36			1.000	4.360	3.900	1.000	1.715	1.994	3.900

3.2. Hydrogen

Pauling's scale is estimated from the bond dissociation energies of two atoms, hydrogen and chlorine, and then arbitrarily extended to all elements not based on the quantitative configuration energy data [3].

Hydrogen has the lowest energy, $E = -13.6$ eV. Batsanov has an experimental covalent radius of 0.37 \AA [30] equal to the Heitler-London's half H-H value R ($R = 0.74 \text{ \AA}$) [26]. Based on these spectroscopic data and the IC model (Equation 2.1.5), we reach its IC value of 2.297 eV and its electronegativity, X_{IC} of 1.333 (Table 2 and Figure 1) that is not that conventionally high as 2.2 .

Table 2. IC and X_{IC} for hydrogen and the top elements.

Elements	Li	Be	H	B	C	N	O	F
IC	1.023	2.064	2.297	3.291	4.302	5.329	6.273	7.37
X_{IC}	0.808	1.237	1.333	1.743	2.167	2.583	2.972	3.423

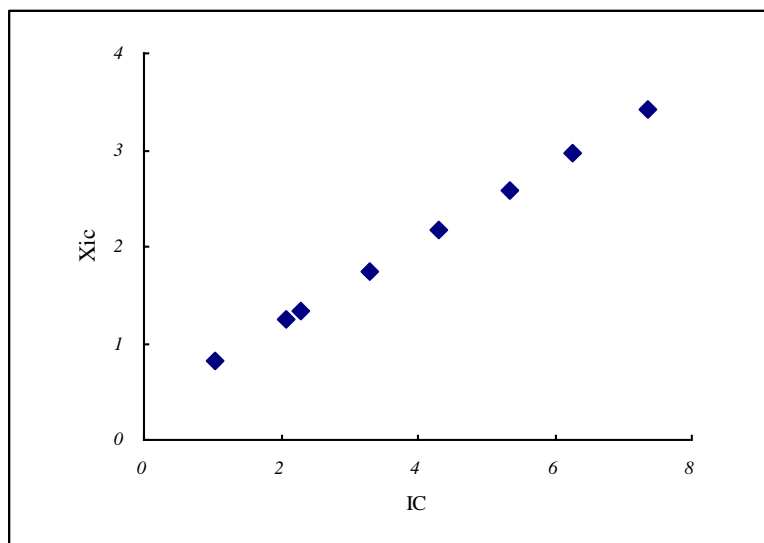
Chart 1. Ionocovalency.

H																	He
(1)2.297																	(2)5.173
Li	Be											B	C	N	O	F	Ne
(1)1.023	(2)2.064											(3)3.291	(4)4.302	(5)5.329	(6)6.273	(7)7.370	(4)6.949
													(2)2.998	(3)4.030	(2)3.648		(2)5.203
Na	Mg											Al	Si	P	S	Cl	Ar
1.130	(2)1.933											(3)2.730	(4)3.371	(5)4.355	(6)5.165	(7)6.048	(4)4.845
												(1)1.585	(2)2.322	(4)3.872	(4)4.093	(5)4.977	(2)3.762
														(3)3.286	(2)2.121	(1)2.851	
K	Ca	Sc	Ti	V	Cr	Mn	Fe	Co	Ni	Cu	Zn	Ga	Ge	As	Se	Br	Kr
(1)0.999	(2)1.617	(3)2.494	(4)3.374	(5)4.359	(6)5.287	(7)6.012	(6)5.520	(4)4.261	(4)4.537	(3)3.918	(2)2.772	(3)3.281	(4)3.895	(5)4.502	(6)5.209	(7)5.941	(6)5.422
			(3)2.824	(4)3.772	(5)4.691	(6)5.426	(5)4.879	(3)3.591	(3)3.802	(2)3.155	(1)2.331	(1)1.841	(2)2.639	(3)3.364	(4)4.090	(5)4.869	(4)4.562
			(2)2.258	(3)3.143	(4)4.058	(5)4.810	(4)4.203	(2)2.874	(2)3.029	(1)2.343				(1)2.422	(2)3.146	(1)2.815	(2)3.538
				(2)2.502	(3)3.395	(4)4.161	(3)3.431	(1)2.113	(1)2.330								
					(2)2.723	(3)3.483	(2)2.786										
					(1)2.077	(2)2.719	(1)2.253										
						(1)2.185											
Rb	Sr	Y	Zr	Nb	Mo	Tc	Ru	Rh	Pd	Ag	Cd	In	Sn	Sb	Te	I	Xe
(1)0.988	(2)1.576	(3)2.332	(4)3.716	(5)4.043	(6)4.964	(7)5.593	(8)6.394	(6)5.450	(5)4.842	(3)3.592	(2)2.658	(3)2.923	(4)3.601	(5)4.057	(6)4.641	(7)5.339	(8)5.553
			(3)2.267	(4)3.575	(5)4.547	(6)5.090	(7)5.890	(4)4.233	(4)4.277	(2)2.973	(1)2.174	(1)1.678	(2)2.472	(3)3.036	(4)3.675	(5)3.817	(6)4.667
			(2)1.884	(3)3.052	(4)3.980	(5)4.563	(6)5.355	(3)3.638	(3)3.672	(1)2.147					(2)2.832	(1)2.530	(4)3.900
				(2)2.532	(3)3.318	(4)4.008	(5)4.791	(2)2.993	(2)3.042								(2)3.044
				(1)2.040	(2)2.760	(3)3.425	(4)4.189	(1)2.287									
					(1)2.155	(2)2.762	(3)3.525										
						(1)2.218	(2)2.924										
Cs	Ba	La	Hf	Ta	W	Re	Os	Ir	Pt	Au	Hg	Tl	Pb	Bi	Po	At	Rn
(1)0.992	(2)1.646	(3)2.185	(4)3.624	(5)4.393	(6)5.178	(7)5.874	(8)6.616	(6)5.683	(6)5.640	(5)5.033	(2)3.118	(3)3.307	(4)3.780	(5)4.273	(6)4.707	(7)5.430	(8)5.567
			(3)3.170	(4)3.924	(5)4.697	(6)5.383	(7)6.122	(5)5.107	(5)5.056	(3)3.965	(1)2.653	(1)1.887	(2)2.574	(3)3.162	(4)3.700	(5)4.419	(6)5.046
			(2)2.691	(3)3.462	(4)4.200	(5)4.881	(6)5.608	(4)4.478	(4)4.518	(2)3.412					(3)3.285	(3)3.522	(4)4.183
				(2)3.056	(3)3.707	(4)4.344	(5)5.066	(3)3.910	(3)3.963	(1)2.689					(2)2.811	(1)2.473	

Chart 1. Cont.

				(1)2.473	(2)3.261	(3)3.795	(4)4.483	(2)3.324	(2)3.405								
						(2)3.237	(3)3.869	(1)2.831	(1)2.749								
						(1)2.597	(2)3.370										
		$\Delta\Delta$					(1)2.779										
Fr	Ra	Ac	Δ	Ce	Pr	Nd	Pm	Sm	Eu	Gd	Tb	Dy	Ho	Er	Tm	Yb	Lu
(1)0.959	(2)1.400	(3)2.093		(4)3.074	(4)3.037	(3)2.572	(3)2.606	(3)2.604	(3)2.385	(3)2.637	(4)3.301	(3)2.730	(3)2.754	(3)2.780	(3)2.829	(3)2.649	(3)2.592
				(3)2.506	(3)2.368	(2)2.050			(2)1.858	(2)2.213	(3)2.686				(2)2.286	(2)2.112	
			$\Delta\Delta$	Th	Pa	U	Np	Pu	Am	Cm	Bk	Cf	Es	Fm	Md	No	Lw
				(4)2.789	(3)2.279	(3)2.316	(4)2.341	(4)2.354	(4)2.349	(3)2.165	(3)2.215	(3)2.229	(3)2.262	(3)2.278	(3)2.309	(3)2.323	(3)3.900
				(3)2.431													

Note: Some ions which might not actually exist are included here just for research reference.

Figure 1. IC vs. X_{IC} for hydrogen and the top elements indicated in Table 2.

The result is strongly supported by the point-charge distribution in hydrides (Table 3) proposed by Mo [33], which shows that in the typical ionic LiH (lithium monohydride) hydrogen gains point charge of 0.783, in the weak ionic BeH (beryllium monohydride) gains only 0.044, but in the covalent BH (boron monohydride) starts to loss point charge. That means that the ionocovalency and the electronegativity of hydrogen are smaller than that of boron. And moreover, the data of electric dipole moments for AlH (aluminum monohydride) (Table 4), proposed by the National Institute of Standards and Technology [34], shows that the aluminum end of the dipole is negative. That means that the ionocovalency and the electronegativity of hydrogen are smaller than that of aluminum.

Table 3. Point-charge distribution q_A and dipole moment.

Hydrides	LiH	BeH	BH	CH	NH	OH	FH
Bond Length (expr)	1.595	1.343	1.233	1.12	1.038	0.971	0.917
Dipole Moment (expr)	5.88	-	-	1.46	-	1.66	1.82
Dipole Moment (calc)	5.999	0.281	-1.689	-1.647	-1.743	-1.864	-2.02
q_A	0.783	0.044	-0.285	-0.306	-0.350	-0.400	-0.459

Table 4. Bond length and dipole moment.

Bond	H-Na	H-Mg	H-Al	H-Si	H-Se	H-P	H-S	H-Cl
Bond Length (expr)	1.887	1.73	1.648	1.52	1.475	1.422	1.341	1.275
Dipole Moment (cal)	5.966	1.231	-0.169	-0.332	-0.634	-0.651	-1.06	-1.468

Hydrogen has one valency orbital and a single electron. It can be an anion to form an ionic bond by gaining another electron and it can be a cation to form a covalent bond by sharing another electron.

Therefore, the IC and the X_{IC} values of hydrogen happen to lie on the border between the weaker ionic beryllium and the weaker covalent boron (Chart 1 and Table 1). We can assign the IC value of hydrogen (2.297) as a standard to estimate the ionocovalent character of the cations. The cations with IC values smaller than that of hydrogen we call the ionic cations and those with IC values greater than that of hydrogen we call the covalent cations. The cations with IC values greater than that of beryllium (2.064) and smaller than that of boron (3.291) we might call borderline cations. The greater the IC than that of hydrogen, the more covalent and the less ionic the cation is, and *vice versa*.

3.3. Diagonal Relationship (Top Periods)

Chart 2 and Chart 3 show that the IC and the X_{IC} scales of the top period rationalize an interesting empirical observation of a similar situation that exists for the pairs of elements. The first element in a given family of the periodic chart tends to resemble the second element in the family to the right as indicated below:

Chart 2. IC -diagonal relationship.

Be ²⁺ (2.252)	B ³⁺ (3.291)	C ⁴⁺ (4.320)	N ⁵⁺ (5.554)	O ⁶⁺ (6.939)
Mg ²⁺ (1.933)	Al ³⁺ (2.730)	Si ⁴⁺ (3.371)	P ⁵⁺ (4.355)	S ⁶⁺ (5.165)

Chart 3. X_{IC} -diagonal relationship.

Be ²⁺ (1.315)	B ³⁺ (1.743)	C ⁴⁺ (2.167)	N ⁵⁺ (2.675)	O ⁶⁺ (3.246)
Mg ²⁺ (1.184)	Al ³⁺ (1.418)	Si ⁴⁺ (1.776)	P ⁵⁺ (2.181)	S ⁶⁺ (2.515)

Chart 4. I_{av} -diagonal relationship.

Be ²⁺ (13.76)	B ³⁺ (23.800)	C ⁴⁺ (37.015)	N ⁵⁺ (53.406)	O ⁶⁺ (72.020)
Mg ²⁺ (11.325)	Al ³⁺ (17.763)	Si ⁴⁺ (25.763)	P ⁵⁺ (35.358)	S ⁶⁺ (46.077)

Chart 5. n^*/r_c -diagonal relationship.

Be ²⁺ (2.238)	B ³⁺ (2.488)	C ⁴⁺ (2.618)	N ⁵⁺ (2.803)	O ⁶⁺ (3.015)
Mg ²⁺ (2.119)	Al ³⁺ (2.189)	Si ⁴⁺ (2.449)	P ⁵⁺ (2.701)	S ⁶⁺ (2.806)

The reason for this relationship is that the pairs of element have approximately similar ionocovalency, $IC = I(I_{av})C(n^*r_c^{-1})$, due to the approximately similar ionic function $I(I_{av})$ (Chart 4) and covalent function $C(n^*r_c^{-1})$ (Chart 5). Because of the electron configuration nature of the elements, the downwards vertical trend in decreasing covalency r_c^{-1} is the opposite of the downwards vertical trend in increasing principal quantum number n^* , and in this section of the Periodic Table the two opposing trends in $C(n^*r_c^{-1})$ approximately cancel each other, resulting in similar values of ionicity, $I(I_{av})$.

3.4. Carbon, Sulfur, P-elements and Hydrogen

There are some arguments about the values of electronegativities of carbon, sulfur, selenium, tellurium, iodine and hydrogen [22]. Chart 1 shows IC values in the order:

$$Se^{2+} (3.146) > S^{2+} (3.121) > C^{2+} (2.998) > Te^{2+} (2.832) > I^+ (2.530) > H^+ (2.297)$$

The results are consistent with the observations that hydrides H_2Se , H_2S , H_2C , H_2Te and HI form H_3O^+ ions in water [35].

As Thomas reviewed, the electronegativity of carbon and sulfur in most of the scale are almost identical. The key point, however, so far as their role as poisons is concerned, is that they differ markedly in the distance at which they sit on the nickel overlayers [36]. The calculations for these locations show that sulfur is very much stronger than carbon as a poison.

The results are also consistent with the experiment data of the dipole moment, which indicates that the electron clouds on the C-S and C-I bond in the molecules CS_2 and Cl_4 are close to the sulfur end and the iodine end, respectively [37]. From *IC* model data (Chart 4), we can see that S^{6+} has a greater ionicity than that of C^{4+} : I_{av} ($\text{S}^{6+} = 46.077$, $\text{C}^{4+} = 37.015$), although they have the close spatial covalency, $n^*r_c^{-1}$ ($\text{C}^{4+} = 2.618$, $\text{S}^{6+} = 2.805$) (Chart 5).

3.5. 3d and 4f Electron Inefficient Screening (p-Block)

As Chart 1 and Table 1 show, the *IC* and X_{IC} run the same uneven trend that is expected to decrease down a group with the features in terms of As^{3+} ($IC = 3.364$, $X_{\text{IC}} = 1.773$) and Bi^{3+} ($IC = 3.162$, $X_{\text{IC}} = 1.690$) both having higher than expected values, comparing those of P^{3+} ($IC = 3.286$, $X_{\text{IC}} = 1.741$) and Sb^{3+} ($IC = 3.036$, $X_{\text{IC}} = 1.638$). This apparent anomaly derives from the filling of the 3*d* row prior to gallium and the 4*f* row prior to thallium, both of which lead to higher effective nuclear charges (Table 1) than the previous periods as a result of inefficient screening of the nuclear charge by the 3*d* and 4*f* electrons, respectively.

3.6. Standard Potential Redox E^0 (Transition Elements)

The *IC* values with a trend of decreasing at d^5 and d^{10} agree well with the variation in values of E^0 (M^{2+}/M) [38] as a function of d^n configuration for the first row of transition metals; the d^0 corresponds to $M = \text{Ca}$ (Table 5).

Table 5. Correlation of *IC* with the standard redox potential E^0 (M^{2+}/M).

d^n	0	2	3	4	5	6	7	8	9	10
E^0/V	-2.87	-1.63	-1.18	-0.971	-1.19	-0.44	-0.28	-0.25	0.34	-0.76
<i>IC</i>	1.617	2.258	2.502	2.723	2.719	2.786	2.874	3.029	3.155	2.772

3.7. Inert Pair Effect ($6s^2$ Elements)

The *IC* model, based on the VB approximation's intuitive appeal and determined by covalent radius and ionization energy, is in accord with the relativistic effects with which contributions to the unusual chemistry of the heavier elements are two principal consequences. First, the *s* orbitals become more stable. Second, *d* and *f* orbitals expand and their energies are less.

For the inert pair effect in Tl(I) , Pb(II) , and Bi(III) , the relativistic effects can give a qualitative verbalization: "The *s* orbitals of the heavier elements become more stable than otherwise expected" [39]. In the *IC* model, as Table 6 shows, the effect is attributable to the fact that the bond property in this case is controlled by the ionic function $I(I_z, I_{\text{av}})$. They are more stable in ionic

compounds than in the entirely covalent form. Their IEs for forming higher covalent bonds are too much higher to form a stable hybridizing ionicity I_{av} :

Table 6. Atomic parameters of Tl, Pb and Bi.

Cations	Tl ⁺	<u>Tl²⁺</u>	Tl ³⁺	Pb ²⁺	<u>Pb³⁺</u>	Pb ⁴⁺	Bi ³⁺	<u>Bi⁴⁺</u>	Bi ⁵⁺
I_z	6.11	20.4	29.8	15	32	42.3	25.6	45.3	56
I_{av}	6.11	13.26	18.77	11.21	18.14	24.18	16.63	23.72	30.18
X_{IC}	1.16	1.59	1.75	1.45	1.74	1.94	1.69	1.95	2.15
IC	1.89	2.92	3.31	2.58	3.44	3.78	3.16	3.81	4.27

3.8. Color of Copper, Silver and Gold

According to the relativistic effects: “The s orbitals of the heavier elements become more stable than otherwise expected” [39], we can only give a qualitative overview on the color of gold and silver, but this has nothing to do with the color of copper.

In the IC model, the phenomenon of “the Color of Copper, Silver and Gold” is attributable to the fact that their bond structure is controlled by their ionocovalency dual properties and we can get a satisfactory explanation by the Dual method.

As Table 7 shows, with the increase of the contraction of the s orbital, the outer d orbitals expand and their ionicities I_{av} are decreased from Cu³⁺ via Ag³⁺ to Au³⁺, however, with the increase of their effective principle quantum number n^* the covalency r_c^{-1} decreases from Cu³⁺ to Ag³⁺ but increases from Ag³⁺ to Au³⁺, which causes the spatial covalency $n^*r_c^{-1}$ of Cu³⁺ higher than that of Ag³⁺ but close to Au³⁺, leading to same trend in ionocovalency.

This quantitative trend in their structure and energy nicely reflect their character of color. Copper and gold are the only two elemental metals with a natural color other than gray or silver, which depends on their ionic delocalizing property of “electron sea” that is capable of absorbing and re-emitting photons over a wide range of frequencies. Copper in its liquefied state, a pure copper surface without ambient light, appears somewhat greenish, a characteristic shared with gold.

Table 7. Atomic parameters of Cu, Ag and Au.

Cations	Cu ³⁺	Ag ³⁺	Au ³⁺
n^*	3.45	3.85	4.36
Z^*	4.349	4.81	5.297
r_c	1.11	1.339	1.336
r_c^{-1}	0.901	0.747	0.749
$n^*r_c^{-1}$	3.108	2.875	3.263
I_{av}	21.610	21.227	18.77
X_{IC}	1.885	1.867	2.021
IC	3.918	3.592	3.965

4. Applications

4.1. Covalency Result Is Retrieved

Villesuzanne *et al.* proposed the study: “New considerations on the role of covalency in ferroelectric niobates and tantalites” [23]. Here, covalency means the amount of mixing of oxygen $2p$ and metal d orbitals to form valence bands; it is evaluated quantitatively through the computation of the crystal orbital overlap population (COOP). The energies of Ta $5d$ and Nb $4d$ atomic orbitals are the same in EHTB parameters. The bond lengths are equal too, as found experimentally. The difference in COOP’s occurs because of larger radial extension of Ta $5d$ compared to Nb $4d$ orbitals, leading to a greater overlap with oxygen $2p$ orbitals. The fact that Ta⁵⁺-O bonds are more covalent than Nb⁵⁺-O bonds is due to a larger radial expansion of Ta $5d$ orbitals. This effect is not accounted for in Pauling electronegativity scales [3], which give information on the energy difference between valence orbitals, not on their spatial overlap. The arguments led to the opposite assumption of reference [24] concerning the covalency of Ta⁵⁺-O and Nb⁵⁺-O bonds from Pauling electronegativity X_p : Ta(1.5) < Nb(1.6).

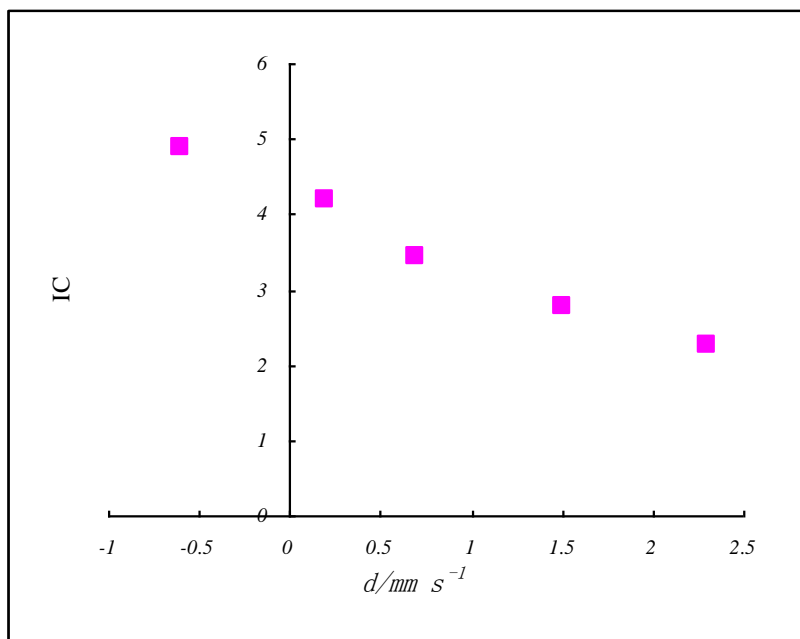
In their later paper, they proposed that the explicit calculation of the electronic structure—COOP’s in particular—gives a larger covalency for Ta⁵⁺-O bonds than for Nb⁵⁺-O bonds. This result is retrieved in the Allred and Rochow scale [7] and in Zhang electronegativity scales for ions [9]. The results can be fairly well accounted in IC model: the energies of Ta $5d$ and Nb $4d$ atomic orbitals are the same in EHTB parameters due to having similar atomic ionicity I_{av} of 24.89 and 27.02, respectively. The bond lengths are equal due to having similar linear covalency r_c^{-1} of 0.745 and 0.745, respectively. The big difference is the spatial covalency, $n^*r_c^{-1}$, in $I(I_{av})C(n^*r_c^{-1}) = n^*(I_{av}/R)^{1/2}r_c^{-1}$. The Ta $5d$ orbitals, compared to Nb $4d$ orbitals, involve greater spatial covalency, $n^*r_c^{-1}$, (Ta⁵⁺ = 3.246, Nb⁵⁺ = 2.869), leading to a greater overlap with oxygen $2p$ orbitals and a greater IC: Ta⁵⁺ (4.393) > Nb⁵⁺ (4.043) and X_{IC} : Ta⁵⁺(2.197) > Nb⁵⁺(2.053).

4.2. Mössbauer Parameters δ and Δ

As the IC model, $n^*(I_{av}/R)^{1/2}r_c^{-1}$, is defined as ionocovalent density of the effective nuclear charges at covalent boundary, it is strongly related with the Mössbauer parameters δ and Δ [40,41]. The value of the isomer shift, δ , depends particularly on the density of s electrons at the nucleus. Therefore, in iron-57 an increase in electron density causes a negative isomer shift; since d electrons tend to shield the nucleus slightly from the s electrons, the value of δ falls as the number of d electrons in the iron atom falls. Mean values of δ [42], Z^* and IC for some oxidation states of iron are shown in Table 8 and Figure 2.

Table 8. IC, Z^* and δ for Iron-57.

Iron-57	Fe ^I	Fe ^{II}	Fe ^{III}	Fe ^{IV}	Fe ^V
$\delta/\text{mm s}^{-1}$	2.3	1.5	0.7	0.2	−0.6
$Z^* = n^*(I_{av}/R)^{1/2}$	2.624	3.245	3.997	4.896	5.684
$IC = n^*(I_{av}/R)^{1/2}r_c^{-1}$	2.253	2.786	3.431	4.203	4.879

Figure 2. IC vs. δ for iron-57 as indicated in Table 9.

4.3. Effective Polarizing Power and Fajans Rules

Fajans suggested the rules to estimate the extent to which a cation could polarize an anion and thus induce covalent character. This Fajans phenomenon happens to be the IC -potential, the ionocovalency, the effective ionic potential (or the effective polarizing power), $n^*(I_{av}/R)^{1/2}r_c^{-1}$.

The simple form of the ionic potential considered the valence charge of the ion with respect to its size. The valence charge is numerically equal to the number of valence electrons of the ion. In some cases we may consider the effective nuclear charge Z^* . For two ions of the same actual nuclear charge, Hg^{2+} and Ca^{2+} , the Hg^{2+} has the higher effective nuclear charge Z^* (4.490) and the IC (3.118), it is considerably more polarizing and its compounds are considerably more covalent than those of Ca^{2+} which has the smaller effective nuclear charge Z^* (2.807) and the IC (1.617). So we have their related melting points $\text{HgCl}_2 = 276$ and $\text{CaCl}_2 = 772$. Comparisons of more compounds are listed in Table 9 (below).

4.4. Melting Points and Bond Properties

Table 9 shows that for the covalent bonding, the increased covalent bonding resulting from increasing the ionicity I_{av} , the σ -covalency r_c^{-1} or the spatial covalency $n^*r_c^{-1}$ can lower the transition temperatures. The melting points decrease with increasing the covalency r_c^{-1} and the spatial covalency $n^*r_c^{-1}$.

However, for ionic bonding (see 4.5.), the ionic compounds are characterized by very strong IC potentials holding the ions together. Increasing the ionic function $I(Z^*, I_{av})$ tends to increase the lattice energy of a crystal. For compounds which are predominantly ionic, increased ionic function $I(Z^*, I_{av})$ or covalent function $C(r_c^{-1}, n^*r_c^{-1})$ will result in increased melting points.

Table 9. Parameters and melting points.

Compound	Cation	Z*	I _{av}	r _c ⁻¹	n*r _c ⁻¹	X _{IC}	IC	Melt.pt (°C) [43]
KF	K ⁺	1.949	4.34	0.513	1.769	0.799	0.999	880°
AgF	Ag ⁺	2.874	7.58	0.747	2.875	1.271	2.147	435°
CaCl ₂	Ca ⁺²	2.807	9.005	0.576	1.987	1.053	1.617	772°
HgCl ₂	Hg ⁺²	4.49	14.82	0.694	3.008	1.672	3.118	276°
CaCl ₂	Ca ⁺²	2.807	9.005	0.576	1.987	1.053	1.617	772°
BeCl ₂	Be ⁺²	2.002	13.76	1.125	2.238	1.315	2.252	405°
NaBr	Na ⁺	1.777	5.14	0.636	1.838	0.853	1.13	755°
MgBr ₂	Mg ⁺²	2.637	11.33	0.733	2.119	1.184	1.933	700°
AlBr ₃	Al ⁺³	3.303	17.76	0.826	2.388	1.512	2.73	97.5°
KBr	K ⁺	1.949	4.34	0.513	1.769	0.799	0.999	730°
CaBr ₂	Ca ⁺²	2.807	9.005	0.576	1.987	1.053	1.617	765°
CsF	Cs ⁺	2.332	3.89	0.41	1.787	0.781	0.956	684°
BaF ₂	Ba ⁺²	3.26	7.605	0.505	2.201	1.065	1.646	1280°

4.5. Lattice Energy

The IC model Equation 2.1.5 is correlated with the electrostatic energy of a cation in Born-Landé equation of the lattice energy

$$U = -Z^2 e^2 AN / 4\pi\epsilon_0 r (1 - n^{-1}) \quad (4.5.1)$$

The both equations reveal how ionic bond strengths vary with the cation ionic charges and inversely with the distance between ions in the lattice. The IC gives a reasonable correlation to the lattice energy as shown in Table 10 and Table 11.

4.6. Lowis Acid Strengths

As we have described [8–10], the stability of a metal complex (the strength of metal-ligand bond) should be a function of the electron-attraction power of the metal. The IC value agrees fairly well with the lattice energy and the crystal field stabilization energy (CFES):

Table 10. Parameters and lattice energies, –U.

Compound	Cation	Z*	I _{av}	r _c ⁻¹	n*r _c ⁻¹	X _{IC}	IC	U(kJmol ⁻¹) [44]
LiH	Li ⁺	1.253	5.39	0.816	2.238	0.808	1.023	905.4
NaH	Na ⁺	1.777	5.14	0.636	1.838	0.853	1.13	810.9
KH	K ⁺	1.949	4.34	0.513	1.769	0.799	0.999	714.2
AgF	Ag ⁺	2.874	7.58	0.747	2.875	1.271	2.147	954
NaF	Na ⁺	1.777	5.14	0.636	1.838	0.853	1.13	903.9
KF	K ⁺	1.949	4.34	0.513	1.769	0.799	0.999	801.2
AgCl	Ag ⁺	2.874	7.58	0.747	2.875	1.271	2.147	904
TlCl	Tl ⁺	2.922	6.11	0.646	2.815	1.164	1.887	732
KCl	K ⁺	1.949	4.34	0.513	1.769	0.799	0.999	697.9
RbCl	Rb ⁺	2.134	4.18	0.455	1.75	0.787	0.97	677.8

Table 11 shows that the IC values correlate with the lattice energies derived from Born-Haber cycle data for MCl_2 where M is a first row d -block metal; the point for d^0 corresponds to $CaCl_2$. (Data are not available for scandium where the stable oxidation state is +3) [38].

Table 11. Lattice energies U (kJmol^{-1}) for MCl_2 correlate with IC .

d^n	0	2	3	4	5	6	7	8	9	10
U	2260	2500	2580	2580	2550	2650	2700	2790	2840	2760
IC	1.617	2.258	2.502	2.723	2.719	2.786	2.874	3.029	3.155	2.772

Crystal field stabilization energy ($CFES$) causes to d level an effect upon thermodynamic stability of complex ions. Owing to the overall contraction in size on traversing a period from left to right, there is an increase in $CFES$ from Ca^{2+} to Zn^{2+} and same trend occurred in IC and X_{IC} . For weak-field ligands (Table 12), the formation constants $\log \beta$ [38] follow the uneven trend and the IC and X_{IC} run in same way: $Mn^{2+} < Fe^{2+} < Co^{2+} < Ni^{2+} < Cu^{2+} < Zn^{2+}$.

Table 12. Values of $\log \beta$ for complexes of 1st row metal ions.

	Mn^{2+}	Fe^{2+}	Co^{2+}	Ni^{2+}	Cu^{2+}	Zn^{2+}
IC	2.719	2.786	2.874	3.029	3.155	2.772
X_{ic}	1.507	1.535	1.571	1.635	1.687	1.529
$\log \beta$ for $[M(en)_3]^{2-}$	5.7	9.5	13.8	18.6	18.7	12.1
$\log \beta$ for $[M(EDTA)]^{2-}$	13.8	14.3	16.3	18.6	18.7	16.1

This order is some time called Irving-Williams series, and is often used in discussing metalloenzyme stabilities (e.g., bioinorganic chemistry).

5. Dual Method

We couldn't expect "*verbum sat sapienti*", but we have a dual parameter group that can dialectically serve many purposes. When IC and X_{IC} correlate with some properties, their dual component parameters and sub-models would give some reason to an observation or find some clue to a new idea. See above all parameters, sub-models and observations to which we have applied the Dual Method. Further examples are as follows:

5.1. An Interesting Comparison

Table 13. Parameters and melting points.

Compound	Cation	Z^*	I_{av}	r_c^{-1}	$n^*r_c^{-1}$	X_{IC}	IC	Melt.pt ($^{\circ}C$) [43]
KBr	K^+	1.949	4.34	0.513	1.769	0.799	0.999	730
CaBr ₂	Ca^{+2}	2.807	9.005	0.576	1.987	1.053	1.617	765
CsF	Cs^+	2.332	3.89	0.41	1.787	0.781	0.956	684
BaF ₂	Ba^{+2}	3.26	7.605	0.505	2.201	1.065	1.646	1280

In Table 13 an interpretation for an interesting comparison can be made between the predominantly ionic species CsF and BaF₂ and the more covalent species KBr and CaBr₂. For ionic species, the bond strengths are controlled by the ionic function $I(I_{av})$. Doubling the I_{av} from 3.890 to 7.605 in the highly

ionic fluorides produces the expected increase in lattice energy and correspondingly doubles the transition temperatures (from 684 °C to 1,280 °C). For covalent bonding, the covalent function $C(n^*r_c^{-1})$ is controlling factor. The little change in covalency r_c^{-1} : 0.513, 0.576 and spatial covalency $n^*r_c^{-1}$: 1.769, 1.987 produces the expected little change in transition temperatures (from 730 °C to 765 °C), despite the doubling of I_{av} from 4.340 to 9.345.

5.2. “Inverted” Sodium-Lithium Electronegativity

Table 14 shows why electronegativity of sodium is higher than that of lithium. When we correlate IC or X_{IC} with lattice energies, there is the “inverted” sodium-lithium electronegativity [8,9,45]; that Li^+ has unexpectedly low values of IC and X_{IC} . However, we can ask $I(I_{av}, Z^*)$ and $C(n^*, r_c^{-1})$ to dialectically explain it: after 1st filling of p orbitals, Na^+ reaches a much higher effective nuclear charge $Z^*(1.777)$ than that of $Li^+(1.253)$. The spatial covalency $n^*r_c^{-1}$ ($Na^+ = 1.838$, $Li^+ = 1.624$) does not cancel the higher effective nuclear charge Z^* anymore. Dialectically, however, Li^+ still has higher ionicity, $I_{av}(5.390)$ and covalency $r_c^{-1}(0.816)$ than that of $Na^+(I_{av} = 5.140, r_c^{-1} = 0.636)$ although covalency is not so important in lattice energy.

Table 14. Parameters and lattice energies, $-U$.

Compound	Cation	Z^*	I_{av}	r_c^{-1}	$n^*r_c^{-1}$	X_{IC}	IC	U (kJmol ⁻¹) [44]
LiH	Li^+	1.253	5.39	0.816	2.238	0.808	1.023	905.4
NaH	Na^+	1.777	5.14	0.636	1.838	0.853	1.13	810.9
KH	K^+	1.949	4.34	0.513	1.769	0.799	0.999	714.2

5.3. Predicting Raw Material for InN Nanocrystals

Changzheng *et al.* [46] presented an effective synthetic protocol to produce high quality InN nanocrystals using indium iodide (InI_3). There has been a question: “Is it possible for high-quality InN to be synthesized from indium halides?” The positive answer has been found in their work using InI_3 . Concerning the four kinds of indium halides, InF_3 , $InCl_3$, $InBr_3$, and InI_3 , InI_3 has the strongest covalent ability. As is known, when two atoms form a chemical bond, the greater the difference between the electronegativity values for the two atoms, the more ionic the chemical bond between them [8–10].

According to the IC model, in the effective polarizing power, $n^*(I_{av}/R)^{1/2}r_c^{-1}$, both the effective principle quantum number, n^* , and the covalent radius, r_c , for halogens are increased in the order: $F < Cl < Br < I$ (Table 1). The polarizability of the anion will be related to its “softness”; that is, to the deformability of its electron cloud. Both increasing n^* and r_c will cause this cloud to be less under the influence of the nuclear charge of the anion and more easily influenced by the charge on the cation. So concerning the four kinds of indium halides, InI_3 is more covalent than the other three. And it is possible for high-quality InN to be synthesized from indium iodide (InI_3).

Comparison of melting points for the anion pairs KF/KBr and $CaCl_2/CaBr_2$ from Table 9 can be treated in same way. KBr and $CaBr_2$ are more covalent and have lower melting points than KF and $CaCl_2$ respectively (see 4.4.).

6. Conclusions

Bond properties can be described quantitatively by an atomic dual nature, Ionocovalency (*IC*), which is defined and correlated with quantum-mechanical potential.

Ionocovalency, $n^*(I_{av}/R)^{1/2}r_c^{-1}$, which is a dual ionocovalent function of bond strength, charge distribution, charge density, effective ionic potential, or effective polarizing power, is composed of quantum parameters or sub-models, which in turn exhibit versatile specific bond properties and applications, forming a multiple functional *Dual Method*.

The *Dual Method* of multiple-functional prediction of that the dual properties of ionocovalency, which is a bridge of the chemical bond and the potential, should be able to explain fairly well the chemical observations of elements throughout the Periodic Table because they are based on the electron configuration and spectroscopy from 1s to nf.

Ionocovalency will be further tested against accurate experimental results and in our later papers we shall apply ionocovalency to discuss the types of chemical bonds, the Lewis acid strengths and the glass crosslink density with the Dual Method. And we believe more new applications will be followed by our colleagues.

References

1. Lewis, G.N. The Atom and the Molecule. *J. Am. Chem. Soc.* **1916**, *38*, 762–785.
2. Pauling, L. *The Nature of the Chemical Bond and the Structure of Molecules and Crystals: An Introduction to Modern Structural Chemistry*, 2nd ed.; Cornell University Press: Ithaca, NY; USA, 1940.
3. Pauling, L. The Nature of the Chemical Bond IV. The energy of single bonds and the relative electronegativity atoms. *J. Am. Chem. Soc.* **1932**, *54*, 3570–3582.
4. Mulliken, R.S. A New Electroaffinity Scale; Together with Data on Valence States and on Valence Ionization Potentials and Electron Affinities. *J. Chem. Phys.* **1934**, *2*, 782.
5. Gordy, W.A. New Method of Determining Electronegativity from Other Atomic Properties. *Phys. Rev.* **1946**, *69*, 604.
6. Sanderson, R.T. Electronegativities in inorganic chemistry. III. *J. Chem. Educ.* **1955**, *31*, 238.
7. Allred, E.G.; Rochow, A.L. A scale of electronegativity based on electrostatic force. *J. Inorg. Nucl. Chem.* **1958**, *5*, 264–268.
8. Zhang, Y. Electronegativity from Ionization Potentials. *J. Mol. Sci. (Chinese)* **1981**, *1*, 125.
9. Zhang, Y. Electronegativities of Elements in Valence States and Their Applications.1. Electronegativities of Elements in Valence States. *Inorg. Chem.* **1982**, *21*, 3886.
10. Zhang, Y. Electronegativities of Elements in Valence States and Their Applications.2. A Scale for Strengths of Lewis Acids. *Inorg. Chem.* **1982**, *21*, 3889.
11. Huheey, J. M. *Inorganic Chemistry: Principles of Structure and Reactivity*, 3rd ed.; Harper and Row: New York, NY, USA, 1983; pp. 140–160.
12. Mullay, J. *Structure & Bonding*; Springer-Verlag Berlin Heidelberg: New York, NY, USA, 1987; pp. 1–25.
13. Datta, D. *Ab initio* calculation, electronegativity equalization and group electronegativity. *Proc. Indian Acad. Sci. (Chem. Sci.)* **1988**, *6*, 549–557.

14. Allen, L.C. Electronegativity is the average one-electron energy of the valence-shell electrons in ground-state free atoms. *J. Am. Chem. Soc.* **1989**, *111*, 9003.
15. Luo, Y.-R.; Benson, S.W. A new electronegativity scale. 12. Intrinsic Lewis acid strength for main-group elements. *Inorg. Chem.* **1991**, *30*, 1676.
16. Zhen, N.W.; Li, G.-S. Electronegativity: Average Nuclear Potential of the Valence Electron *J. Phys. Chem.* **1994**, *98*, 3964.
17. Bergmann, D.; Hinze, J. Electronegativity and Molecular Properties. *J. Angew. Chem. Int. Ed.* **1996**, *35*, 150–163.
18. Cherkasov, A.R.; Galkin, V.I.; Zueva, E.M.; Cherkasov, R.A. The concept of electronegativity and the current state of the problem. *Russ. Chem. Rev.* **1998**, *5*, 375–392.
19. Mackay, K.M.; Mackay, R.A.; Henderson, W. *Introduction to Modern Inorganic Chemistry*, 6th ed.; Nelson Thornes: Cheltenham, UK, 2002; pp. 53–55.
20. Portier, J.; Campet, G.; Etoumeau, J.; Shastry, M.C.R.; Tanguy, B. A simple approach to materials design: Role played by an ionic-covalent parameter based on polarizing power and electronegativity. *J. Alloys Compd.* **1994**, *209*, 59–64.
21. Lenglet, M. Iono-covalent character of the metal-oxygen bonds in oxides: A comparison of experimental and theoretical data. *Act. Passive Electron. Compon.* **2004**, *27*, 1–60.
22. Li, Z.-H.; Dai, Y.-M.; Wen, S.-N.; Nie, C.-M.; Zhou, C.-Y. Relationship between atom valence shell electron quantum topological indices and electronegativity of elements. *Acta Chimica Sinica.* **2005**, *14*, 1348.
23. Villesuzanne, A.; Elissalde, C.; Pouchard, M.; Ravez, J. New considerations on the role of covalency in ferroelectric niobates and tantalates. *Eur. Phys. J. B* **1998**, *6*, 307.
24. Ravez, J.; Pouchard, M.; Hagenmuller, P. Chemical bonding and ferroelectric perovskites. *Eur. J. Solid State Inorg. Chem.* **1991**, *25*, 1107.
25. Lower, S. Why atoms don't collapse. In *Chem1 Virtual Textbook*; Available online: <http://www.chem1.com/acad/webtext/virtualtextbook.html> (accessed on 18 October 2010).
26. Duffy, J.A. *General Inorganic Chemistry*, 2nd ed.; Longmans: London, UK, 1974; pp. 19–20.
27. Blaber, M. *General Chemistry 1 Virtual Textbook, Web Course Tutorial*; Available online: www.mikeblaber.org/oldwine/chm1045/chm1045.htm (accessed on 18 October 2010).
28. Mackay, K.M.; Mackay, R.A.; Henderson, W. *Introduction to Modern Inorganic Chemistry*; 6th ed.; Nelson Thornes: Cheltenham, UK, 2002; pp. 45–46.
29. Pauling, L. Atomic Radii and Interatomic Distances in Metals. *J. Am. Chem. Soc.* **1947**, *69*, 542.
30. Batsanov, S.S. Experimental determination of covalent radii of elements. *Russ. Chem. Bull.* **1995**, *12*, 2245–2250.
31. Cordero, B.; Gomez, V.; Platero-Prats, A.E.; Reves, M.; Echeverris, J.; Cremades, E.; Barragan F.; Alvarez, S. Covalent Radius. *Dalton Trans.* **2008**, 2832–2838.
32. Rappe, A.K.; Casewit, C.J.; Colwell, K.S.; Goddard, W.A., III; Skiff, W.M. UFF, a full periodic table force field for molecular mechanics and molecular dynamics simulations. *J. Am. Chem. Soc.* **1992**, *114*, 10024–10035.
33. Mo, Y.-R. Tow issues on the polarity of chemical bond. *Univ. Chem.* **1993**, *4*, 15.
34. Computational Chemistry Comparison and Benchmark Database. Available online: <http://cccbdb.nist.gov/default.htm> (accessed on 18 October 2010).

35. Dalian Technology Institute. *Inorg. Chem. (in Chinese)*, 3rd ed.; High Education Press: Beijing, China, 1990; pp. 638, 804.
36. Thomas, J.M. *Principles and Practice of Heterogeneous Catalysis*; Wiley-VCH: Weinheim, Germany, 1996; p. 448.
37. Xu, G.-X. *Material Structure (in Chinese)*; People's Education Press: Beijing, China, 1961; p. 160.
38. Housecroft, C.E. Sharepe, A.G. *Inorganic Chemistry*, 2nd ed.; Pearson Education: Harlow, UK, 2005.
39. Pyykkö, P. Relativistic Effects in Structural Chemistry. *Chem. Rev.* **2002**, *3*, 563–594.
40. Reguera, E.; Bertran, J.F.; Miranda, J.; Portilla, C. Study of the dependence of Mossbauer parameters on the outer cation in nitroprussides. *J. Radioanal. Nucl. Chem. Lett.* **1992**, *3*, 191–201.
41. Reguera, E.; Rodriguez-Hernandez, J.; Champi, A.; Duque, J.G.; Granado, E.; Rettori, C. Unique coordination of copper in hexacyanometallates. *Zeitschrift für physikalische chemie* **2006**, *12*, 1609–1619.
42. Heslop, R.B.; Jones, K. *Inorganic Chemistry*; Elsevier Scientific Publishing: Amsterdam, The Netherland, 1976; p. 31.
43. Mackay, K.M.; Mackay, R.A.; Henderson, W. *Introduction to Modern Inorganic Chemistry*, 6th ed.; Nelson Thornes: Cheltenham, UK, 2002; p. 120.
44. Huheey, J.E. *Inorganic Chemistry: Principles of Structure & Reactivity*, 2nd ed.; Harper and Row Publishers: New York, NY, USA, 1978; p. 93.
45. Lambert, C.; Kaupp, M.; von Rague Schleyer, P. "Inverted" sodium-lithium electronegativity: polarity and metalation energies of organic and inorganic alkali-metal compounds. *Organometallics* **1993**, *12*, 853–859.
46. Wu, C.; Li, T.; Lei, L.; Hu, S.; Liu, Y.; Xie, T. Indium nitride from indium iodide at low temperatures: Synthesis and their optical properties. *New J. Chem.* **2005**, *29*, 1610.

© 2010 by the authors; licensee MDPI, Basel, Switzerland. This article is an open access article distributed under the terms and conditions of the Creative Commons Attribution license (<http://creativecommons.org/licenses/by/3.0/>).